Optimal Power Flow with Power Flow Routers

Junhao Lin, *Student Member, IEEE,* Victor O. K. Li, *Fellow, IEEE,* Ka-Cheong Leung, *Member, IEEE,* and Albert Y.S. Lam, *Member, IEEE*

***Abstract*—Power flow routing is an emerging control paradigm for the dynamic control of electric power flows. In this paper, we propose a generic model of a power flow router (PFR) and incorporate it into the optimal power flow (OPF) problem. First, a generic PFR architecture is proposed to encapsulate the desired functions of PFRs. Then, the load flow model of PFRs is developed and incorporated into the OPF framework. To pursue global optimality of the non-convex PFR-incorporated OPF (PFR-OPF) problem, we develop a semidefinite programming (SDP) relaxation of PFR-OPF. By introducing the regularization terms that favor a low-rank solution and tuning the penalty coefficients, a rank-1 solution can be obtained and used for recovering an optimal or near-optimal solution of the PFR-OPF and the results are verified in numerical tests. The efficacy of the PFR-OPF framework allows us to investigate the impact of PFR integration. With the system loadability as an example, the numerical results show that remarkable enhancement can be achieved by installing PFRs at certain critical buses of the network.**

***Index Terms*—power flow routers, optimal power flow, convex relaxation, semidefinite programming.**

NOMENCLATURE

Sets

$\mathcal{N}$	Index set of buses.
$\mathcal{E}$	Index set of transmission lines.
Ω_i	Index set of one-hop neighbors of Bus i.
$\mathbf{X}$	Set of decision variables of the non-convex PFR-OPF problem.
$\widehat{\mathbf{X}}$	Set of decision variables of the relaxed PFR-OPF problem.
$\mathcal{J}_m$	The mth bag of tree decomposition.
$\mathcal{I}_m$	Set of matrix variable $\mathbf{W}$'s diagonal entries that correspond to the branch terminal voltages of the buses/PFRs in bag $\mathcal{J}_m$.
$\mathcal{L}_s$	Index set of transmission lines selected for penalization.

Parameters

y_{ik}	Transmission line admittance of Branch (i,k).
g_{ik}	Line conductance of Branch (i,k).
b_{ik}	Line susceptance of Branch (i,k).
c_{ik}	Shunt capacitance of Branch (i,k).
$U_{i,min}$	Lower bound of bus voltage V_i.
$U_{i,max}$	Upper bound of bus voltage V_i.
$T_{i_k,min}$	Lower bound of transformer ratio T_{i_k} of PFR i in Branch (i,k).
$T_{i_k,max}$	Upper bound of transformer ratio T_{i_k} of PFR i in Branch (i,k).
$\beta_{i_k,min}$	Lower bound of phase shift β_{i_k} of PFR i in Branch (i,k).
$\beta_{i_k,max}$	Upper bound of phase shift β_{i_k} of PFR i in Branch (i,k).
$\gamma_{i_k,max}$	Upper bound of series voltage tap ratio γ_{i_k} of PFR i in Branch (i,k).
$Q_{Ci_k,min}$	Lower bound of reactive power compensation Q_{Ci_k} of PFR i in Branch (i,k).
$Q_{Ci_k,max}$	Upper bound of reactive power compensation Q_{Ci_k} of PFR i in Branch (i,k).
$S_{ik,max}$	Upper bound of the magnitude of complex power flow of Branch (i,k).
ε_r	Penalty coefficient for regularization.
ε_s	Penalty coefficient for apparent power losses.

Variables

V_i	Voltage of Bus i or voltage of common bus of PFR i.
V_{i_k}	Branch terminal voltage of PFR i in Branch (i,k).
T_{i_k}	Transformer ratio of PFR i in Branch (i,k).
β_{i_k}	Phase shift of PFR i in Branch (i,k).
γ_{i_k}	Tap ratio of series voltage injection of PFR i in Branch (i,k).
Q_{Ci_k}	Reactive power compensation of PFR i in Branch (i,k).
S_i	Complex power of aggregate local power injection of Bus/PFR i.
S_{ik}	Complex power flow from Bus/PFR i to Bus/PFR k.
$\mathbf{V}$	Column vector obtained by stacking all the branch terminal voltage variables.
$\mathbf{W}$	Auxiliary matrix variable corresponding to vector of branch terminal voltage $\mathbf{V}$.
W_{i_k}	Diagonal entry of matrix variable $\mathbf{W}$ corresponding to branch terminal voltage V_{i_k}.
$W_{i_k l_m}$	Off-diagonal entry of matrix variable $\mathbf{W}$ corresponding to branch terminal voltages V_{i_k} and V_{l_m}.
W_i	Auxiliary variable corresponding to bus voltage V_i.
Π_{i_k}	Auxiliary variable corresponding to transformer ratio T_{i_k}.
Γ_{i_k}	Auxiliary variable corresponding to series voltage tap ratio γ_{i_k}.

This research is supported in part by the Theme-based Research Scheme of the Research Grants Council of Hong Kong, under Grant No. T23-701/14-N. A.Y.S. Lam was also supported in part by the Seed Funding Programme for Basic Research of The University of Hong Kong under Grant 201601159009.

The authors are with the Department of Electrical and Electronic Engineering, The University of Hong Kong, Pokfulam, Hong Kong (e-mail: {jhlin, vli, kcleung, ayslam}@eee.hku.hk).

h_r	Regularization function.
L_{ik}	Apparent power loss over the series impedance of Branch (i, k).
λ	Loading factor.

I. Introduction

The increase in energy demand and the integration of renewable energy sources (RESs) are stressing the grid, prompting system operators to take active control measures for managing the power flow more efficiently and intelligently. Traditional power flow controls may no longer be suitable for the future power system operation because of their limited control range and slow dynamic response [1]. Due to the development of power electronics over the past two decades [1]–[3], power flow routing [2], [4], [5], an emerging control paradigm for the dynamic and responsive control of power flows, is a promising solution for power flow control.

Power flow controllers (PFCs) and power flow routers (PFRs) are the building blocks of power flow routing. In this paper, we propose a generic model of PFRs and an optimal power flow (OPF) framework for the analytical study of power flow routing. We will explain our motivation and identify the research gap by reviewing the state-of-the-art.

The need for a smarter and more resilient grid has led to continuous innovations on PFCs [1]–[3] and PFRs [4], [6], [7], but the literature does not usually make a clear distinction between PFCs and PFRs. To avoid ambiguity, we use PFR to refer to a control device that is able to manage multiple incoming/outgoing power flows, while PFC refers to a device that can only actively adjust the power flow through one transmission line or appliance. Hence, a PFC is part of a PFR. In general, PFCs [1]–[3] control the branch power flow by modifying the parameters of a transmission line, such as series injection of the voltage source and/or resistance, and shunt reactive power compensation. PFRs are useful for interconnecting multiple transmission lines and interfacing appliances at different power levels [4], [6], [7]. The energy router [6] and the solid-state transformer (SST) [7] only focus on interfacing various types of local power injections, but they are not designed for controlling branch power flows.

We can see that most existing research efforts on PFCs and PFRs have been devoted to the hardware implementation [1]–[3], [6], [7], whereas [4] does focus on the generic model of a PFR. However, the PFR model proposed in [4] is just a simple combination of a computational unit and several PFCs, and it is only applicable to the distribution network. The lack of a generic functional model of PFRs has hindered network-level research on power flow routing. To overcome this, we propose a generic PFR model that covers the necessary and desired functions of a PFR so as to facilitate a theoretical study of power flow routing in the power network.

We focus on the modelling of PFRs for power system optimization. Although the research on load flow models of PFCs is rich [3], [5], [8], [9], existing work on the modelling of PFRs is rather limited. Flexible AC transmission system (FACTS) devices [3], the best known PFCs, have been studied extensively for improving asset utilization [5], [8], [9]. A sensitivity method has been employed in [5] to analyze the impact of PFCs on corrective power flow control. However, due to the inherent complexity of the method, reactive power is not considered in [5]. In general, a PFC adjusts the power flow by its series and/or shunt sources injected over the transmission line [3]. The change of power flow induced by the series source of the PFC is usually converted to and modelled as power injections to both buses of the branch [5], [8], [9], since the approach preserves the symmetry of the admittance matrix and the structure of the Jacobian matrix. Different from the literature, we develop the load flow model of a PFR characterized by "branch terminal voltages," the terminal voltages of the PFR, which is a more intuitive approach to formulate the power flow according to the PFR's operating principle.

We further incorporate the PFR model into the OPF framework. The OPF problem determines the optimal operating points for a power system in terms of a global objective function, subject to the network physics, such as Kirchhoff's circuit laws, as well as the engineering limits of the state and control variables of the system, such as inequality constraints on transmission line flows, power generations, and configurations of control devices [10], [11]. In the proposed PFR model, the voltage of a conventional bus is augmented and evolves into multiple branch terminal voltages to reduce the coupling among corresponding power flows. As a result, the size of the PFR-incorporated OPF (PFR-OPF) problem is proportional to the number of branches, and comparable to the conventional OPF problem whose size is proportional to the number of buses since the power network is in general a sparse graph. Hence, existing nonlinear programming (NLP) solvers, such as interior point methods used in our numerical tests, are still able to obtain a local optimal solution of the non-convex PFR-OPF problem. Although the existing power injection method [5], [8], [9] and the model proposed in this paper are not essentially different since they both aim to model the control abilities of PFCs and PFRs, the proposed PFR model is more amenable for applying the convex relaxation to the PFR-OPF problem. In the power injection method, the series injected source of PFC introduces nonlinear terms which are not easy to relax, especially for those characterizing the phase-shifting effect.

In general, the alternating-current (AC) OPF problem is challenging due to its non-convexity and usually very large problem size [10]. The non-convexity stems from the nonlinear power flow equation due to Kirchhoff's laws, as well as the nonlinear or even discrete characteristics of some control variables, such as tap-changing transformers [10], [12]. The problem size can be very large in the real-world industrial application not only because of the scale of the power system, but also more significantly due to the number (tens of thousands or more) of postulated contingencies [10], [12]. In the literature, various approaches have been proposed to tackle those respective challenges [10], [13]. Many nonlinear programming (NLP) approaches, such as quadratic programming, Lagrangian relaxation, heuristic algorithms, and interior-point methods, have been proposed to cope with the non-convexity [10], [13]. In order to solve the security-constrained OPF

(SCOPF) with a large number of contingencies efficiently, various classes of approaches, including iterative contingency selection schemes, decomposition methods, and network compression, have been developed [12], [14]. Some of them are mature and capable of finding at least the local optimum of large-scale SCOPF problems with up to 3000 buses [14] or even 9000 buses and 12000 contingencies [12].

In this research, we only consider the basic and continuous scenarios of the AC OPF problem, and do not include contingencies and discrete variables. With such simplifications, this paper aims to address the non-convexity introduced by Kirchhoff's laws as well as PFCs and PFRs, and pursues global optimality of the PFR-OPF problem through convex relaxation. However, it is worth pointing out that the computational challenges induced by the security constraints and the discrete variables can be formidable as both the numbers of contingencies and discrete variables can be huge, thousands or more in the real-world industrial OPF problems. Therefore, in the industrial practice, given the stringent time constraint to provide a solution, achieving global optimality of the OPF solution is often not the primary concern since it can be too time-consuming [14]. Although the solution method for the OPF problem proposed in this paper is not designed to address the large-scale SCOPF problem, we expect that the proposed PFR-OPF framework is extensible to incorporate the security constraints. In fact, due to their fast-response capability, PFCs and PFRs can be very powerful resources to perform post-contingency corrective control [5]. The flexible SCOPF framework proposed in [5] incorporates PFCs into the corrective SCOPF problem, while the ability to handle a large contingency set is not discussed. When the PFCs and PFRs are treated as re-dispatchable resources in the corrective SCOPF problem, the coupling effect among their post-contingency decision variables would be a new challenge due to the nonlinear control regions of PFCs and PFRs, especially for the phase shifting effect. Hence, existing methods for the large-scale SCOPF problem, such as contingency selection and decomposition [12], [14], may not be applicable directly. It is an important problem and will be our future work.

In recent years, there have been extensive research efforts to develop convex relaxation methods for the conventional OPF problems in pursuit of the global optimality [15]–[23]. The main focus of these convex relaxation methods in [15]–[23], similar to our work, is to tackle the non-convexity due to Kirchhoff's laws, and thus they do not consider discrete variables. Among these proposals, only [18] studies the SCOPF problem but it does not account for a large contingency set. While the local solution techniques usually find the global optimal solutions in practice [14], they may fail to converge or converge to a local optimum [13], [24]. Moreover, they are unable to guarantee global optimality of the solutions. The second-order cone programming (SOCP) relaxation is able to globally solve the OPF problems for the radial networks that satisfy certain technical conditions [17], [23]. The semidefinite programming (SDP) relaxation has received much research attention [15], [18], [19], [21] since it is able to obtain the global optimal or near-optimal solutions for a broad class of meshed networks. Voltage phasors can be recovered successfully from the solution if the rank of its matrix variable is equal one. While the structure of feasible region and the existence of local optima may render the SDP relaxation unable to produce a physically meaningful solution [24], penalization [18], [19] and Laplacian-based [21] approaches have been proposed to encourage a rank-1 solution so that a feasible and globally near-optimal solution to the original non-convex OPF problem can be obtained for many test cases, including some large networks with up to 3000 buses. Recently, the SDP relaxation have been generalized to a family of "moment relaxation" [16], [20], [22] which is essentially a polynomial optimization approach and seeks to attain tighter relaxation by gradually increasing the order of relaxation if the lower-order relaxations fail. While higher-order moment relaxations are able to globally solve a broader class of OPF problems comparing to the first-order relaxation, i.e., the SDP relaxation, the computational cost grows very quickly as the relaxation order increases [16]. Therefore, sparsity-exploiting technique [20] has been proposed to reduce the computational burden. And penalization approach [22] has also been adopted to improve numerical performance when a near-optimal solution is obtained.

To pursue global optimality of the PFR-OPF problem, we derive an SDP relaxation of the original problem. While there is much research on the convex relaxation of the conventional OPF problem [15]–[23] as discussed, we found no existing work that applies it to an OPF problem with PFCs or PFRs. The convex relaxation for the PFR-OPF poses a new challenge that has not been studied before. Since the relationship among the terminal voltages of a PFR is highly nonlinear and non-convex due to the enhanced voltage controllability, it is difficult to construct a relaxation that preserves such coupling and leads to an exact solution for successful recovery of voltage phasors. While it has been shown that the SDP relaxation is able to handle variable real transformer ratios and shunt elements [15], the exact relaxation for the series injected source of PFC and PFR, such as the phase shifter, has not been tackled yet. In fact, existing research on the SOCP relaxation [17] assumes that phase shifters possess unlimited phase-shifting capabilities or their capabilities would not be the binding constraints so as to avoid incorporating the nonlinear phase-shifting effect into the OPF problem. However, this ideal assumption may not always hold. In this research, we account for the capability of phase shifters and model the phase-shifting effect explicitly in PFR-OPF problem as well as its SDP relaxation. It is achieved by relaxing part of the coupling constraints and incorporating the regularization terms that favor an exact solution into the objective function. As verified in our numerical tests, such regularization helps improve the quality of the solution significantly while it only has a negligible effect on the optimal value of the original objective. In addition, we show excellent compatibility of the proposed PFR model in the sense that existing techniques for improving the performance of the SDP relaxation, such as the penalization method to solicit a low-rank solution [18], [19], and the graph-theoretic decomposition method to reduce the computational complexity [18], can naturally be adapted to our PFR-OPF framework. Although the SDP relaxation may

fail to find a physically meaningful solution for a few power networks with certain configurations as studied in [20], [22], [24], the remedial approaches [18], [19] adopted are able to improve its quality of solutions significantly and broaden its range of applicable cases, such as the network with up to 3000 buses as evaluated in our numerical study in Section V. The generalization of the SDP relaxation for the PFR-OPF problem into the higher-order moment relaxation is an ongoing research and remains challenging since the phase-shifting effect would render the rectangular representation of voltage variables in the moment relaxation [16], [20], [22] nonlinear and hence difficult to relax as the relaxation order goes above one. Nonetheless, we consider that this research may serve as the initial efforts to apply convex relaxation to the OPF problem with a set of nonlinear control variables for voltages.

To summarize, we propose a generic PFR model and an OPF framework incorporating PFRs. Our contributions are listed as follows:

- The proposed PFR model encapsulates the desired features of PFRs, and is amenable for implementation and for the theoretical study of power flow routing.
- The load flow model of PFRs is developed and incorporated successfully into the OPF framework for power flow analysis and grid optimization.
- We derive a computationally efficient SDP relaxation of the PFR-OPF problem and design the regularization method to facilitate a rank-1 solution. The benefit of PFRs in enhancing the system loadability is evaluated by the proposed framework.

This paper extends our prior work [25] with substantial differences and improvements as follows:

- This paper improves the PFR model by designing a generic formulation of the branch terminal voltages so as to adapt the model to various grid components including conventional buses and PFCs.
- This paper solves the PFR-OPF problem through an SDP relaxation, which is more realistic than the SOCP relaxation in [25], which requires a sufficient number of ideal phase shifters to ensure exact relaxation.
- This paper compares the results of the non-convex and relaxed PFR-OPF problems, and analyzes the quality of the SDP solution by varying the penalty coefficients.

The remainder of this paper is structured as follows. In Section II, the generic architecture of the PFR model is proposed. In Section III, the load flow model of PFRs is developed and incorporated into the OPF framework. Then, the PFR-OPF problem is relaxed and solved through the SDP relaxation in Section IV. Case studies are presented and the numerical results are analyzed in Section V. Finally, Section VI draws the conclusions.

II. Generic Model of Power Flow Routers

A PFR can manage all of its incoming/outgoing power flows intelligently, and coordinate with other grid components to maintain the system stability. In general, a PFR should achieve the following functions:

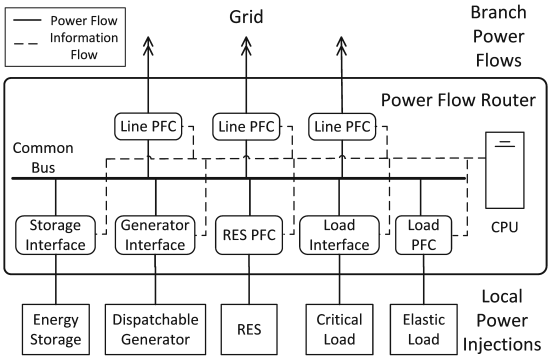

Fig. 1. Proposed architecture of a power flow router.

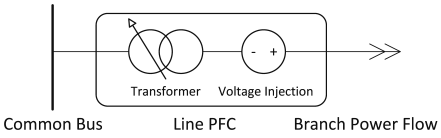

Fig. 2. Functional schematic of a line power flow controller.

- interconnection and coordination of multiple bidirectional branch power flows at different voltage levels;
- autonomous control of individual branch power flows;
- independent control of the active and reactive power flows for each branch;
- supporting various types of interfaces for local power injections at different voltage and power levels;
- voltage regulation and reactive power compensation; and
- power buffering and energy storage.

Based on the above design objectives, we propose a generic architecture of PFR as shown in Fig. 1. Existing designs of PFR [4], [6], [7] can be viewed as some particular embodiments of the proposed architecture. Two major types of power flows, namely, branch power flows from/to other PFRs/buses, and local power injections, are injected to a PFR. Within the PFR, all power flows share a "common bus," which is analogous to the conventional bus, after passing through the respective PFCs or interfaces. The control capabilities of PFCs enable the autonomous control of the corresponding power flows.

The "line PFC," whose functional schematic is shown in Fig. 2, connects the external transmission line to the common bus of the PFR, and controls the corresponding branch flow. The line PFC consists of a controllable transformer and a series-injected voltage source. The transformer is used to adjust the voltage of the branch power flow to the same level as that of the common bus. Primary control of the power flow is achieved by controlling the series-injected voltage source, similar to the control mechanism of some existing PFCs, such as the unified power flow controller (UPFC) [3].

The local power injections are categorized into five types, namely, energy storage, dispatchable generation, intermittent RES, critical load, and elastic load. Energy storage acts as an energy buffer. The RES power is interfaced by the "RES PFC" which regulates the RES power, such as reactive

power compensation and voltage regulation. Local demand is classified into the critical load and the elastic load. The former has to be met in real time while the latter may be a deferrable load or a non-critical load managed by the "load PFC". The "load PFC" that interconnects the common bus and the elastic load can be an electric spring [26] to regulate the common bus voltage and absorb the fluctuations of the RES power. The energy storage, dispatchable generator, and critical load would be connected to the common bus through respective interfaces.

The operations of the PFCs and interfaces are coordinated by a central processing unit (CPU) which is the central controller of the PFR. PFRs can also communicate and coordinate with each other via some other controllers in the network.

It should be noted that the architecture given in Fig. 1 is an ideal configuration. A practical PFR may sacrifice certain power flow control capability to strike a balance between the control capacity and the cost of the device.

III. Load Flow Model and Optimal Power Flow

A. Load Flow Model of Power Flow Router

The load flow model of a PFR is developed based on the PFR model discussed in Section II. Consider a power network with N buses modelled as a connected undirected graph, denoted by $\mathcal{G} = (\mathcal{N}, \mathcal{E})$ with the bus set $\mathcal{N} := \{1, 2, \ldots, N\}$ and the set of transmission lines or branches $\mathcal{E} \subseteq \mathcal{N} \times \mathcal{N}$. A branch $(i,k) \in \mathcal{E}$ with its two terminal buses $i, k \in \mathcal{N}$ is modelled by the equivalent π circuit with the line admittance $y_{ik} = g_{ik} + \mathrm{j}b_{ik}$, where $g_{ik} \geq 0$ and $b_{ik} \leq 0$ denote the conductance and susceptance of branch (i,k), respectively, and the shunt capacitance $c_{ik} = c_{ki} \geq 0$ as illustrated in Fig. 3. Denote the set of one-hop neighbors of each bus $i \in \mathcal{N}$ as $\Omega_i \subseteq \mathcal{N}$. Note that Branch (i,k) and Branch (k,i) are regarded as the same branch since $\mathcal{G}$ is undirected.

By abuse of notation, we denote the PFR installed at Bus $i \in \mathcal{N}$ as PFR i. The branch power flows and the local power injections of Bus i are interfaced to PFR i. The common bus of PFR i is characterized by the voltage $V_i \in \mathbb{C}$ analogous to that of a conventional bus, with the operation range given as:

$$U_{i,min} \leq |V_i| \leq U_{i,max} \tag{1}$$

where the operator $|\cdot|$ takes the magnitude.

For each one-hop connected Bus/PFR $k \in \Omega_i$ of PFR i, we define a "branch terminal voltage" $V_{i_k} \in \mathbb{C}$, indicating the terminal voltage of PFR i for Branch (i,k). According to Fig. 2, the relationship between the common bus voltage V_i and the branch terminal voltage V_{i_k} can be modelled by:

$$V_{i_k} = T_{i_k} \mathrm{e}^{\mathrm{j}\beta_{i_k}} (1 + \gamma_{i_k}) V_i, \tag{2}$$

where $\beta_{i_k} \in \mathbb{R}$ is the phase shift of the transformer, and $T_{i_k} \in \mathbb{R}$ represents the transformer ratio. Moreover, as a common practice for the series voltage compensation [1], [3], we assume that the series voltage that the line PFC can inject is a fraction $\gamma_{i_k} \in \mathbb{C}$ of the voltage $T_{i_k} e^{\mathrm{j}\beta_{i_k}} V_i$, which is equal to the grid-side voltage of the line PFC when the series voltage compensation is zero. In addition, the line PFC, as a power electronic device, of PFR i in branch (i,k) may possess

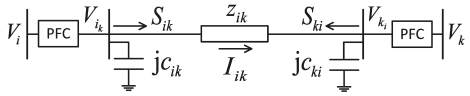

Fig. 3. Notations for a branch (i,k).

certain extra capability of reactive power compensation which is modelled by the reactive power injection $Q_{Ci_k} \in \mathbb{R}$. The controllable ranges of T_{i_k}, β_{i_k}, γ_{i_k}, and Q_{Ci_k} are constrained by respective upper and lower bounds as follows:

$$T_{i_k,min} \leq T_{i_k} \leq T_{i_k,max} \tag{3}$$

$$\beta_{i_k,min} \leq \beta_{i_k} \leq \beta_{i_k,max} \tag{4}$$

$$0 \leq |\gamma_{i_k}| \leq \gamma_{i_k,max} \tag{5}$$

$$Q_{Ci_k,min} \leq Q_{Ci_k} \leq Q_{Ci_k,max} \tag{6}$$

where $\gamma_{i_k,max} \in [0,1]$ characterizes the capability of the series voltage injection.

Denote the complex power flow from PFR i to Bus/PFR $k \in \Omega_i$ as $S_{ik} = P_{ik} + \mathrm{j}Q_{ik}$ which satisfies Ohm's law as:

$$S_{ik} = V_{i_k}(V_{i_k} - V_{k_i})^* y_{ik}^* - \mathrm{j}\,|V_{i_k}|^2 c_{ik} \tag{7}$$

where * denotes the conjugate operator of a complex number.

Symmetrically, the branch terminal voltage V_{k_i} on the other end of Branch (i,k) and the complex power flow S_{ki} are modelled as:

$$V_{k_i} = T_{k_i} \mathrm{e}^{\mathrm{j}\beta_{k_i}} (1 + \gamma_{k_i}) V_k \tag{8}$$

$$S_{ki} = V_{k_i}(V_{k_i} - V_{i_k})^* y_{ik}^* - \mathrm{j}\,|V_{k_i}|^2 c_{ki} \tag{9}$$

Let $S_i = P_i + \mathrm{j}Q_i$ denote the complex power of the aggregate local power injection of PFR i. Then, if the conversion losses of the line PFCs are neglected, the power balance equation for PFR i is formulated as:

$$S_i = \sum_{k \in \Omega_i} S_{ik}. \tag{10}$$

From (7) and (9), the branch power flows S_{ik} and S_{ki} are controlled by the terminal voltages V_{i_k} and V_{k_i} of the two buses/PFRs on both ends. According to (2), for a fixed common bus voltage V_i, each terminal voltage $\{V_{i_k} | k \in \Omega_i\}$ of PFR i can be controlled autonomously by the corresponding line PFC. On the other hand, the PFR is more than a simple aggregation of a number of PFCs since the terminal voltages of the PFCs in a PFR are not completely independent and are actually coupled weakly by the common bus voltage. This feature is characterized by the proposed PFR model. PFRs enable larger controllable ranges of the branch terminal voltages than the voltages of the conventional buses. Hence, the achievable region of branch power flows of PFRs is greater than those of conventional buses. The enlarged control regions contribute to reduction of transmission losses, relief of grid congestion, and improvement of power transfer capability.

Since the focus of this study is on the modelling and optimization of branch power flows, we do not go into details on the load flow models of the local power injections. In this paper, we only consider the simple power injection models of conventional generators and critical loads as formulated

in Section V-A. Nonetheless, existing sophisticated power injection models, such as the smart load model [27], can be incorporated directly into the PFR model.

The load flow model of PFR given in (1)–(10) is versatile and applicable to various types of grid components, including conventional buses and PFCs, by setting proper lower and upper bounds of the parameters in (3)–(6).

B. PFR-Incorporated Optimal Power Flow

The load flow model of PFR developed in Section III-A will be incorporated into the OPF problem. The OPF with PFRs is different from the conventional OPF since the bus voltage has evolved into several branch terminal voltages when the PFR is attached to the bus. Define the set of the variables as:

$$\begin{aligned}\mathbf{X} :=&\{(S_i, V_i)|i \in \mathcal{N}\} \cup \{(S_{ik}, S_{ki}, V_{i_k}, V_{k_i}, T_{i_k}, T_{k_i},\\ &\beta_{i_k}, \beta_{k_i}, \gamma_{i_k}, \gamma_{k_i}, Q_{Ci_k}, Q_{Ck_i})|(i,k) \in \mathcal{E}\}.\end{aligned} \tag{11}$$

We minimize a global objective function f of the power network, subject to the power balance constraints at PFRs/buses, the constraints for the control regions of PFRs, and the constraints for branch power flows. The general form of the PFR-incorporated OPF (PFR-OPF) is formulated as follows:

$$\min_{\mathbf{X}} f \tag{12a}$$

subject to

$$|S_{ik}|, |S_{ki}| \leq S_{ik,max}, \forall (i,k) \in \mathcal{E} \tag{12b}$$

$$(1),\ (10),\ \forall i \in \mathcal{N} \tag{12c}$$

$$(2)\text{–}(7),\ \forall i \in \mathcal{N}, k \in \Omega_i \tag{12d}$$

The constraint in (12b) specifies the upper limits of the branch flow magnitude to protect transmission lines. Candidates for the scalar function f can be any economic or operational evaluation of the system, such as the generation cost or the system loadability which will be studied in Section V.

The PFR-OPF problem in (12) extends the conventional OPF problem by augmenting the controllable ranges of the conventional buses. Therefore, the PFR-OPF problem is non-convex and non-deterministic polynomial-time hard (NP-hard) like the conventional OPF [15] due to the non-convex feasible region of power flows determined by (7) and (10). Moreover, the PFR-OPF problem entails a higher computational complexity than the conventional OPF problem because of the increase in the problem size and the nonlinear relation between the common bus voltage and the branch terminal voltage as indicated in (2). Nonetheless, since the power network in general is sparse with a small edge-to-vertex ratio, the increase in the problem size from the order of the number of buses to that of the number of branches is almost linear.

IV. Convex Relaxation

A. Semidefinite Programming Relaxation

Inspired by the methods proposed in [15], [18], [19] for convexifying the conventional OPF problem, we propose a method to relax the PFR-OPF problem in (12) into an SDP problem to seek the global optimal solution.

We introduce the auxiliary matrix variable $\mathbf{W} \in \mathbb{C}^{2E\times 2E}$ corresponding to the branch terminal voltages as:

$$\mathbf{W} := \mathbf{V}\mathbf{V}^* \tag{13}$$

where $\mathbf{V} \in \mathbb{C}^{2E}$ is defined as a column vector obtained by stacking the paired voltages V_{i_k} and V_{k_i} for every branch $(i,k) \in \mathcal{E}$. If $\mathbf{W}$ replaces $\mathbf{V}$ in the PFR-OPF problem in (12), there are at least two additional constraints to be included in the formulation so that $\mathbf{V}$ can later be recovered from $\mathbf{W}$. The first constraint is $\mathbf{W} \succeq 0$, which means $\mathbf{W}$ is positive semidefinite. The second one is $\mathrm{rank}\{\mathbf{W}\} = 1$, which means the rank of $\mathbf{W}$ is equal to one. Without this rank constraint, the original non-convex power flow region determined by (7) and (10) is relaxed into a convex region. However, different from the existing studies [15], [18], [19] on the SDP relaxation for the conventional OPF problem, such relaxation does not suffice to render the PFR-OPF problem convex due to the highly nonlinear relationship between the common bus voltage and the branch terminal voltage of a PFR modelled in (2).

To tackle this issue, we develop a relaxation method which can not only preserve the coupling between the terminal voltages of the PFR but also produce a rank-1 solution $\mathbf{W}_{opt}$ for successful recovery of the voltage phasors. For ease of presentation, we label the diagonal entries of $\mathbf{W}$ as:

$$W_{i_k} := |V_{i_k}|^2, \forall i \in \mathcal{N}, k \in \Omega_i, \tag{14}$$

and the off-diagonal entries of $\mathbf{W}$ as:

$$W_{i_k l_m} := V_{i_k} V_{l_m}^*, \forall i, l \in \mathcal{N}, k \in \Omega_i, m \in \Omega_l \tag{15}$$

Then, taking the magnitude squared of (2), we get:

$$W_{i_k} = \Pi_{i_k} \Gamma_{i_k} W_i \tag{16}$$

where W_i, Π_{i_k}, and Γ_{i_k} are defined as:

$$W_i := |V_i|^2, \forall i \in \mathcal{N} \tag{17}$$

$$\Pi_{i_k} := T_{i_k}^2, \forall i \in \mathcal{N}, k \in \Omega_i \tag{18}$$

$$\Gamma_{i_k} := |1 + \gamma_{i_k}|^2, \forall i \in \mathcal{N}, k \in \Omega_i \tag{19}$$

Note that the angle variable β_{i_k} in (2) disappears after we determine its magnitude. According to (3) and (5), the feasible regions of Π_{i_k} and Γ_{i_k} are convex. Hence, (3), (5), and (16) can be combined into one constraint as follows:

$$\begin{aligned}T_{i_k,min}^2(1-\gamma_{i_k,max})^2 W_i \leq W_{i_k}\\ \leq T_{i_k,max}^2(1+\gamma_{i_k,max})^2 W_i, \forall i \in \mathcal{N}, k \in \Omega_i\end{aligned} \tag{20}$$

Constraint (20) is convex since the feasible region of W_i is linear according to (1) and (17).

To account for the phase-shifting angle variable β_{i_k} in (2) and Constraint (4) while ensuring convexity, we propose to limit the angular difference between any two branch terminal voltages of the same bus/PFR by:

$$\theta_{i_k i_l,min} \leq \angle W_{i_k i_l} \leq \theta_{i_k i_l,max}, \forall i \in \mathcal{N}, k \neq l \in \Omega_i, \tag{21}$$

where $\theta_{i_k i_l,min}$ and $\theta_{i_k i_l,max}$ are the lower and upper bounds, respectively, of the angular difference $\angle W_{i_k i_l}$ between V_{i_k} and V_{i_l}. Due to the stability concern, a large phase shift between the two branch terminal voltages should be avoided. Hence, we assume that $\angle W_{i_k i_l} \in [-\frac{\pi}{2}, \frac{\pi}{2}]$, which also makes Constraint

(21) convex. Then, we can derive the values of $\theta_{i_k i_l,min}$ and $\theta_{i_k i_l,max}$ based on (2)–(5) as follows:

$$\begin{aligned}\theta_{i_k i_l,min} := \max\{&\beta_{i_k,min} - \beta_{i_l,max} - \arcsin\gamma_{i_k,max} \\ &- \arcsin\gamma_{i_l,max}, -\frac{\pi}{2}\}, \forall i \in \mathcal{N}, k \neq l \in \Omega_i.\end{aligned} \tag{22}$$

$$\begin{aligned}\theta_{i_k i_l,max} := \min\{&\beta_{i_k,max} - \beta_{i_l,min} + \arcsin\gamma_{i_k,max} \\ &+ \arcsin\gamma_{i_l,max}, \frac{\pi}{2}\}, \forall i \in \mathcal{N}, k \neq l \in \Omega_i.\end{aligned} \tag{23}$$

From (21)–(23), we have $\mathrm{Re}\{W_{i_k i_l}\} \geq 0$, where $\mathrm{Re}\{\cdot\}$ is the operator for getting the real part. Thus, Constraint (21) can be explicitly expressed in the convex form as follows:

$$\begin{aligned}&\mathrm{Re}\{W_{i_k i_l}\}\tan\theta_{i_k i_l,min} \leq \mathrm{Im}\{W_{i_k i_l}\} \\ &\leq \mathrm{Re}\{W_{i_k i_l}\}\tan\theta_{i_k i_l,max}, \forall i \in \mathcal{N}, k \neq l \in \Omega_i,\end{aligned} \tag{24}$$

where $\mathrm{Im}\{\cdot\}$ is the operator for getting the imaginary part.

Then, we derive a constraint to account for the coupling between W_i and $W_{i_k i_l}$. According to (21)–(23), we have:

$$\cos\angle W_{i_k i_l} \geq \cos(\max\{|\theta_{i_k i_l,min}|, |\theta_{i_k i_l,max}|\}) \tag{25}$$

According to (2)–(5), we can obtain:

$$|W_{i_k i_l}| \geq W_i T_{i_k,min} T_{i_l,min} (1 - \gamma_{i_k,max})(1 - \gamma_{i_l,max}) \tag{26}$$

Note that $\cos\angle W_{i_k i_l} = \frac{\mathrm{Re}\{W_{i_k i_l}\}}{|W_{i_k i_l}|}$. Hence, from (25) and (26), we can obtain the relationship between W_i and $W_{i_k i_l}$ as:

$$\begin{aligned}&\mathrm{Re}\{W_{i_k i_l}\} \geq W_i T_{i_k,min} T_{i_l,min} (1 - \gamma_{i_k,max})(1 - \gamma_{i_l,max}) \\ &\cos(\max\{|\theta_{i_k i_l,min}|, |\theta_{i_k i_l,max}|\}), \forall i \in \mathcal{N}, k \neq l \in \Omega_i\end{aligned} \tag{27}$$

We have developed the convex constraints (20), (24), and (27) to relax the non-convex constraint (2) and to account for the operation range of the PFR specified in (3)–(5). However, they are still not sufficient to make the optimal solution $\mathbf{W}_{opt}$ of the relaxed problem to be rank-1, since PFR enlarges the controllable ranges of its branch terminal voltages. Thus the off-diagonal entries $W_{i_k i_l}, \forall i \in \mathcal{N}, k \neq l \in \Omega_i$, related to PFR i are only coupled weakly with the diagonal entries of $\mathbf{W}$. Under such circumstance, most numerical algorithms tend to result in the highest-rank SDP solution, even though a rank-1 solution may exist. To address this issue, we introduce a regularization term h_r that favors a low-rank solution to the original objective function f. As discussed in [18] and [28], a penalty function that minimizes a weighted sum of the diagonal entries as well as maximizes a weighted sum of the off-diagonal entries $W_{i_k i_l}, \forall i \in \mathcal{N}, k \neq l \in \Omega_i$, can serve this purpose. Therefore, we formulate the regularization function h_r as follows:

$$h_r := \sum_{i \in \mathcal{N}} \sum_{k < l \in \Omega_i} (W_{i_k} + W_{i_l} - W_{i_k i_l} - W_{i_l i_k}) \tag{28}$$

We summarize the SDP relaxation for the PFR-OPF problem. Define the penalty coefficient for the regularization h_r as $\varepsilon_r \geq 0$. We also define the set of the variables of the relaxed PFR-OPF problem as:

$$\begin{aligned}\widehat{\mathbf{X}} :=&\{\mathbf{W}\} \cup \{(S_i, W_i) | i \in \mathcal{N}\} \cup \{(S_{ik}, S_{ki}, \\ &Q_{Ci_k}, Q_{Ck_i}) | (i,k) \in \mathcal{E}\}.\end{aligned} \tag{29}$$

The relaxed PFR-OPF problem is formulated as follows:

$$\min_{\widehat{\mathbf{x}}} f + \varepsilon_r h_r \tag{30a}$$

subject to

$$S_i = \sum_{k \in \Omega_i} (S_{ik} + \mathrm{j} Q_{Ci_k}), \forall i \in \mathcal{N} \tag{30b}$$

$$S_{ik} = (W_{i_k} - W_{i_k k_i}) y_{ik}^* - \mathrm{j} W_{i_k} c_{ik}, \forall i \in \mathcal{N}, k \in \Omega_i \tag{30c}$$

$$U_{i,min}^2 \leq W_i \leq U_{i,max}^2, \forall i \in \mathcal{N} \tag{30d}$$

$$Q_{Ci_k,min} \leq Q_{Ci_k} \leq Q_{Ci_k,max}, \forall i \in \mathcal{N}, k \in \Omega_i \tag{30e}$$

$$|S_{ik}|, |S_{ki}| \leq S_{ik,max}, \forall (i,k) \in \mathcal{E} \tag{30f}$$

$$\mathbf{W} \succeq 0 \tag{30g}$$

and (20), (24), (27) (30h)

Note that for a conventional bus i without a PFR or PFC, the corresponding penalty in (28), $(W_{i_k} + W_{i_l} - W_{i_k i_l} - W_{i_l i_k}), \forall i < l \in \Omega_i$, is kept constant by Constraints (20), (24), and (27). In fact, the regularization $\varepsilon_r h_r$ has a negligible effect on the optimal value of the original objective while it is very effective in yielding a rank-1 $\mathbf{W}_{opt}$. This will be verified by our numerical tests in Section V.

B. Adapted Techniques for Performance Improvement

While the SDP relaxation for the OPF problem can facilitate the search of the global optimum, the number of scalar variables of its semidefinite matrix variable, such as $\mathbf{W}$, grows quadratically with the size of the power network. Besides the issue of high dimensionality, the SDP relaxation may not always result in a rank-1 matrix solution depending on the problem formulation [18], [19] and the values of line admittances [15]. While the relaxed PFR-OPF problem in (30) will also experience these issues, we show that the graph-theoretic decomposition method proposed in [18] for reducing the computational complexity and the penalization method in [18], [19] for soliciting a low-rank solution can be adapted naturally to our PFR-OPF framework to ameliorate the situation.

As discussed in [18], the semidefinite constraint on the square matrix variable related to the bus voltages can be replaced by a set of semidefinite constraints on some principal submatrices of the matrix variable without affecting the optimality of the relaxed problem according to the chordal theorem [29]. The dimensions of those principal submatrices, which are constructed from a tree decomposition of the power network, are much lower than the full matrix variable due to the sparsity of the network [18]. The interested readers may refer to [18] and the references therein for information about the tree decomposition and its algorithm. By adopting the definition and notation of the tree decomposition in [18], we denote the bags of a tree decomposition of the power network as $\mathcal{J}_1, \mathcal{J}_2, \ldots, \mathcal{J}_M \subseteq \mathcal{N}$, where M is the number of bags. Note that each bag $\mathcal{J}_m, m = 1, \ldots, M$, is a subset of the bus set $\mathcal{N}$. Construct the set $\mathcal{I}_m := \{W_{i_k} | i \in \mathcal{J}_m, k \in \Omega_i\}$, which consists of $\mathbf{W}$'s diagonal entries that correspond to the branch terminal voltages of the buses/PFRs in $\mathcal{J}_m, m = 1, \ldots, M$. Let $\mathbf{W}\{\mathcal{I}_m\}$ be the principal submatrix of $\mathbf{W}$ formed by the intersected rows and columns containing the elements in $\mathcal{I}_m$.

Theorem 1: The optimal objective value of the relaxed PFR-OPF problem in (30) does not change if its constraint $\mathbf{W} \succeq 0$ is replaced by the constraints as follows:

$$\mathbf{W}\{\mathcal{I}_m\} \succeq 0, \forall m \in \{1, 2, \ldots, M\}. \tag{31}$$

Proof: This theorem is a direct variant of Part 2 of Theorem 1 in [18] to fit into our PFR-OPF framework. Since the bus voltage has evolved into several branch terminal voltages in the PFR model, we replace the bus-related variables in Part 2 of Theorem 1 in [18] by the branch-related variables in Theorem 1 in this paper. Constraint (31) preserves the structural information of the tree decomposition of the power network. Therefore, the rest of the proof follows from Part 2 of Theorem 1 in [18] and the chordal theorem in [29]. ■

Theorem 1 allows us to reduce the computational complexity of the SDP relaxation remarkably. Take the IEEE 118-bus system [30] as an example. There are 186 branches in the system, and thus $\mathbf{W}$ is a 372×372 matrix. However, the submatrix with the largest size among all of the $M = 117$ submatrices in (31) according to the tree decomposition results is merely a 28×28 matrix which is less than 0.57% of the size of $\mathbf{W}$.

Furthermore, to pursue a rank-1 solution of the SDP relaxation, [19] proposes to penalize the total reactive power generation, and [18] further proposes to penalize the apparent power loss over the series impedance of the transmission lines. While both methods can be incorporated into the PFR-OPF problem easily, we use the latter in this paper since it is formulated by the entries of $\mathbf{W}$ explicitly and allows flexibility to adjust the total penalty by modifying the set of the penalized transmission lines. Similar to [18], define the apparent power loss over the series impedance of Branch (i, k) without incorporating the shunt capacitance as:

$$\begin{aligned} L_{ik} &:= |S_{ik} + \mathrm{j}W_{i_k} c_{ik} + S_{ki} + \mathrm{j}W_{k_i} c_{ki}| \\ &= |W_{i_k} + W_{k_i} - W_{i_k k_i} - W_{k_i i_k}|\,|y_{ik}^*| \end{aligned} \tag{32}$$

Denote the set of branches that are selected for the penalty as $\mathcal{L}_s \subseteq \mathcal{E}$. A convenient and safe choice of $\mathcal{L}_s$ is to make it equal to the branch set $\mathcal{E}$ of the network. [18] also proposes a heuristic method for designing $\mathcal{L}_s$. Define the penalty coefficient for apparent power losses as $\varepsilon_s \geq 0$. We summarize the two adapted techniques for improving the performance of the SDP relaxation and formulate the improved relaxed PFR-OPF problem as follows:

$$\min_{\hat{\mathbf{x}}} f + \varepsilon_r h_r + \varepsilon_s \sum_{(i,k)\in\mathcal{L}_s} L_{ik} \tag{33}$$

subject to (30b)–(30f), (30h), and (31).

The improved relaxed PFR-OPF problem in (33) is modified from the relaxed problem in (30) by adding the penalization term of apparent power losses to the objective function, and replacing the original SDP constraint in (30g) by a set of SDP constraints in (31) according to the tree decomposition results of the power network.

V. Case Study

A. Problem Specification and Performance Metric

We investigate the impact of PFR integration on system loadability. According to [31], the loadability can be assessed by increasing all of the loads by a loading factor $\lambda \geq 0$ until the system reaches the critical state. Therefore, as a specific implementation of the PFR-OPF problem, the local power injections are categorized into the reactive power compensation of the PFRs, the critical loads, the dispatchable generators with the operation ranges as follows:

$$S_i = (P_{Gi} - P_{Li}) + \mathrm{j}(Q_{Gi} - Q_{Li} + \sum_{k\in\Omega_i} Q_{Ci_k}), \forall i \in \mathcal{N} \tag{34}$$

$$P_{Li} + \mathrm{j}Q_{Li} = \lambda(P_{Li0} + \mathrm{j}Q_{Li0}), \forall i \in \mathcal{N} \tag{35}$$

$$P_{Gi,min} \leq P_{Gi} \leq P_{Gi,max}, \forall i \in \mathcal{N} \tag{36}$$

$$Q_{Gi,min} \leq Q_{Gi} \leq Q_{Gi,max}, \forall i \in \mathcal{N} \tag{37}$$

where P_{Gi} and Q_{Gi} denote the active and reactive generations, respectively, of the generator at Bus/PFR $i, i = 1, \ldots, \mathcal{N}$. Their controllable ranges are specified in (36) and (37), respectively. P_{Li} and Q_{Li} denote the active and reactive loads, respectively, at Bus/PFR i. $P_{Li0} \geq 0$ and $Q_{Li0} \in \mathbb{R}$ are the base active and reactive loads, respectively, at Bus/PFR i.

To evaluate the loadability, each of the three versions of the PFR-OPF problems in (12), (30), and (33) is extended by considering $\lambda, P_{Gi}, Q_{Gi}, P_{Li}, Q_{Li}, i = 1, \ldots, \mathcal{N}$, and Constraints (34)–(37). Finally, the objective function f is set as:

$$f = -\sum_{i\in\mathcal{N}} P_{Li} \tag{38}$$

We will assess and compare the loadabilities of the power network under various penetrations and allocations of PFRs and UPFCs [3]. The reason for choosing UPFCs for comparison with PFRs is that the UPFC has similar power flow control capability as the PFR. The UPFC is one of the most versatile PFCs and is able to regulate the bus voltage and control the active and reactive power flow independently [3]. While UPFCs are deployed far less commonly in the real-world power systems compared to some other FACTS devices, such as static shunt compensators (SVCs) [3], due to the currently high costs of UPFCs, existing academic research has explored and demonstrated the benefits of UPFCs in various aspects, such as the enhancement of system stability [32] and reliability [33].

Denote the optimal loading factor as λ_{opt} obtained by solving the PFR-OPF problems for loadability assessment. λ_{opt} will serve as the performance metric.

B. General Setup

In Sections V-D and V-E, numerical tests are performed on the standard IEEE benchmark systems with 30, 57, and 118 buses. The parameter specifications of the three tested systems follow the standard settings archived at [30], except for the branch flow limits of the 57-bus and 118-bus systems which are not given in [30]. Without loss of generality, we set the flow limits of all branches of the test systems with 57 and 118 buses to be 300 MW and 600 MW, respectively,

based on the nominal settings. This set of tests is to investigate the effect of the penalty coefficients ε_r and ε_s of the relaxed problem in (33) on the quality of solutions, and to evaluate the enhancement of loadability with various penetrations of PFCs and PFRs.

Furthermore, in Section V-F, we investigate the tractability of the PFR-OPF problem of large power networks with up to 3000 buses. The test systems are seven models of the Polish power systems included in MATPOWER [34]. The parameter specifications of the test systems in the simulations follow the MATPOWER data sets [34].

In this paper, we follow the standard specifications as much as possible in the numerical tests rather than look for special test cases by varying the parameters, because we would like to focus on the modelling of PFRs and its impact on system loadability, and do not discuss the existence of multiple local optima of the PFR-OPF problem. Nonetheless, it would be of importance and part of the future work to study the influence of PFCs and PFRs on the optimality and the structure of feasible region. In fact, there is no general method to produce a test case with multiple local optima since such locality is sensitive to the parameter specifications and the objective function of the OPF problem [22], [24].

For ease of analysis, we assume that, for every PFR and UPFC, the capability of the series voltage injection $\gamma_{i_k,max} = 0.05$, the limits of the branch reactive power compensation $Q_{Cik,max} = -Q_{Cik,min} = 0.05$ p.u., and the transformer ratios T_{i_k}'s are equal to their respective nominal settings. For every phase shifter, the capability of phase shift is set as $\beta_{i_k,max} = -\beta_{i_k,min} = 5^\circ$. The per-unit base is 100 MVA.

The original non-convex PFR-OPF problem in (12) is solved by the interior point method supported by the NLP solver IPOPT [35]. For each test case, the power flow solution of its nominal setting is fed in as the initial solution of the NLP solver. The test codes are programmed in the Julia language and its optimization packages [36].

The relaxed PFR-OPF problem in (33) is solved by the SDP solver of the Mosek toolbox for MATLAB [37]. The test codes are implemented by CVX [38] in MATLAB.

All the numerical tests were performed in a computer with a quad-core 3.30 GHz processor and 16 GB of RAM.

C. Allocation Scheme for PFCs and PFRs

In our prior work [25], a greedy algorithm for allocating PFRs to enhance the loadability is proposed. We apply the placement algorithm, namely, Algorithm 1, in [25] to determine the locations of the PFCs and PFRs in this study. The numerical results reported in Sections V-D and V-E show that this algorithm can achieve very good results. Since the allocation of PFCs and PFRs is not the focus of the present paper, the details of the placement algorithm are omitted. Interested readers can refer to [25]. There is also other allocation schemes, such as FACTS devices allocation in [31], available in the literature. We expect that our PFR-OPF framework can be extended and incorporated into the existing methods, such as the one in [31]. In this paper, we do not discuss the cost models of PFRs and UPFCs because our focus is on the modelling of power flow routing from an OPF approach. While the cost model of PFRs is not available in the literature, some existing works, such as [39], have analyzed the cost and benefit of PFCs and showed that net financial benefits can be achieved by optimizing the investment and placement of PFCs.

TABLE I
ALLOCATION RESULTS OF PFRS AND UPFCS TO OBTAIN 99.5% OF THE MAXIMUM ACHIEVABLE LOADABILITY

Test System	Scenario	Allocation Result
30-Bus System	2 PFRs	Buses 8, 28
	4 UPFCs	Branches (6,8), (6,28), (8,28), (10,22)
57-Bus System	3 PFRs	Buses 1, 36, 38
	6 UPFCs	Branches (1,15), (13,49), (14,46), (24,25), (37, 38), (44,45)
118-Bus System	5 PFRs	Buses 26, 37, 64, 65, 77
	13 UPFCs	Branches (24,70), (25,26), (26,30), (30,38), (49,66), (59,63), (63,64), (65,68), (68,69), (69,77), (75,118), (83,85), (89,92)

In Sections V-D and V-E, we focus on three scenarios of the system loadability for each of the three IEEE test systems as follows:

- Maximum achievable loadability: It is achieved by installing PFRs at all buses of the system. This scenario will be referred to as "full PFRs."
- 99.5% of the maximum loadability: PFRs or UPFCs are added to the system until the loadability reaches 99.5% of the maximum achievable loadability. This set of scenarios will be referred to as "K_R PFRs" and "K_C UPFCs," where K_R and K_C are the numbers of PFRs and UPFCs, respectively, allocated in the network. Table I summarizes their allocation results of the IEEE systems with 30, 57, and 118 buses applied in the simulations.
- Baseline loadability: No PFR or UPFC is allocated in the system. This scenario will be referred to as "baseline."

Hence, for each of the three test systems, we will compare and report the results of four scenarios regarding the penetrations of PFRs and UPFCs, namely, "Full PFRs," "K_R PFRs," "K_C UPFCs," and "Baseline," in Sections V-D and V-E.

D. Selection of Penalty Coefficients

We investigate the effects of the penalty coefficients ε_r and ε_s of the relaxed problem in (33) on the rank of the optimal solution $\mathbf{W}_{opt}$ and the original objective value which is equivalently evaluated by the loadability λ_{opt}. Since the regularization $\varepsilon_r h_r$ is not required for the conventional OPF problem, we search for an appropriate value of ε_s for the conventional OPF problem first, and then apply the chosen ε_s to find an appropriate ε_r for a rank-1 $\mathbf{W}_{opt}$ under a specific placement of PFRs or UPFCs. Without loss of generality, we make $\mathcal{L}_s$ equal to $\mathcal{E}$ which is most likely to lead to a rank-1 solution according to [18].

Fig. 4 presents the optimal loading factor λ_{opt} and the rank of $\mathbf{W}_{opt}$ under various values of ε_s for apparent power losses with given values of ε_r for regularization. For the results of the IEEE 118-bus system shown in Fig. 4(c), the two curves of "5 PFRs" and "13 UPFCs" almost overlap. As ε_s increases and

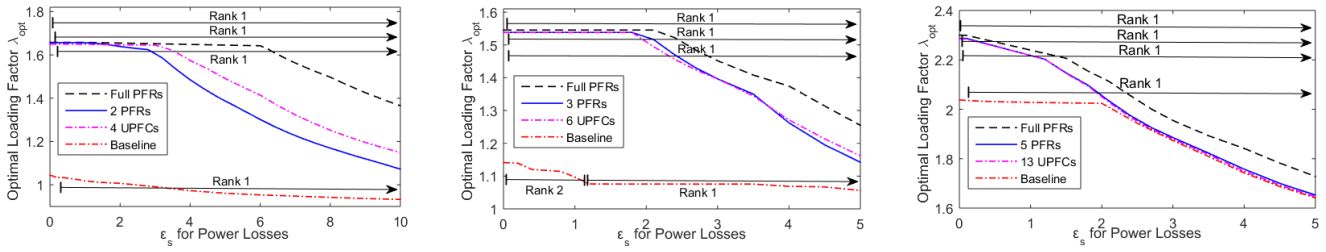

(a) IEEE 30-bus system, $\varepsilon_r = 0.1$ (b) IEEE 57-bus system, $\varepsilon_r = 1$ (c) IEEE 118-bus system, $\varepsilon_r = 1$

Fig. 4. Effects of the values of the penalty coefficient ε_s for apparent power losses on the optimal loading factor λ_{opt} and the rank of the optimal solution $\mathbf{W}_{opt}$ in the three test systems with given values of the penalty coefficient ε_r for regularization.

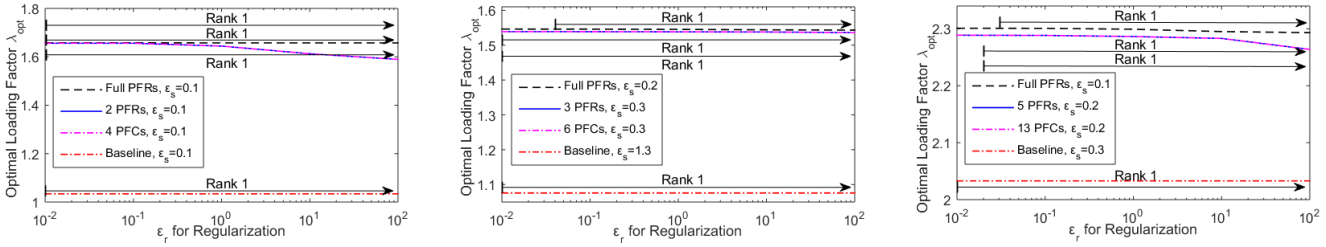

(a) IEEE 30-bus system (b) IEEE 57-bus system (c) IEEE 118-bus system

Fig. 5. Effects of the values of the penalty coefficient ε_r for regularization on the optimal loading factor λ_{opt} and the rank of the optimal solution $\mathbf{W}_{opt}$ in the three test systems with given values of the penalty coefficient ε_s for apparent power losses.

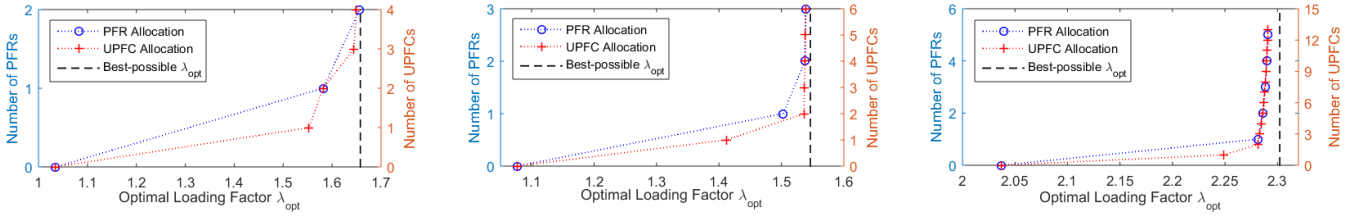

(a) IEEE 30-bus system (b) IEEE 57-bus system (c) IEEE 118-bus system

Fig. 6. Loadability enhancement as the number of allocated PFRs or UPFCs increases. For each of the test systems, PFRs or UPFCs are added to the system until the loadability reaches 99.5% of the maximum achievable loadability.

reaches a certain threshold, $\mathbf{W}_{opt}$ becomes rank-1 while the obtained λ_{opt} experiences non-negligible decrease if ε_s keeps growing. Therefore, the value of ε_s should be chosen carefully to avoid excessive penalization. Furthermore, the greater the penetration rate of PFRs or UPFCs, the less the threshold of ε_s for a rank-1 $\mathbf{W}_{opt}$. The reason is that the voltage control capabilities of the PFRs alleviate the coupling of the cycles of the meshed network and thus make them "easier" for the SDP relaxation to attain a rank-1 solution [19].

Fig. 5 presents the solution λ_{opt} and the rank of $\mathbf{W}_{opt}$ under various values of ε_r for regularization with given values of ε_s for apparent power losses. For each of the three test systems, the two curves of "K_R PFRs" and "K_C UPFCs" almost overlap. The results show that as long as ε_r surpasses a small threshold which is no greater than one for each of the scenarios reported in Fig. 5, the rank of $\mathbf{W}_{opt}$ stays at one. As ε_r grows from 0.01 to 100, λ_{opt} decreases very slowly. In particular, for the IEEE 57-bus system, λ_{opt} remains almost the same when ε_r varies as shown in Fig. 5(b). This suggests that the proposed regularization $\varepsilon_r h_r$ in (33) has almost a negligible effect on the original objective value, and is very efficient in achieving a rank-1 $\mathbf{W}_{opt}$. Moreover, the greater the penetration rates of PFRs or UPFCs, the greater the threshold of ε_r for a rank-1 $\mathbf{W}_{opt}$. This corresponds to our analysis in Section IV-A that the weak coupling among the branch terminal voltages of the line PFCs of a PFR entails the regularization.

E. Loadability Enhancement

The solutions of the original non-convex PFR-OPF problem in (12) and its convex relaxation in (33) are compared and summarized in Table II. Based on the findings in Section V-D, ε_s and ε_r are set to obtain a rank-1 $\mathbf{W}_{opt}$ for the SDP relaxation. The solution λ_{opt} obtained by the original PFR-OPF in (12) is referred to as "λ_{opt} by NLP" because it is solved by the NLP solver. Correspondingly, the solution λ_{opt} obtained by the SDP relaxation is referred to as "λ_{opt} by SDP." "Accuracy" in Table II represents the accuracy of the SDP relaxation, evaluated by "λ_{opt} by SDP" as a percentage of "λ_{opt} by NLP." "Enhancement" represents the percentage improvements of loadability compared to the baseline scenarios where no PFR or UPFC is available.

As shown in Table II, the optimal loading factor λ_{opt} obtained by the SDP relaxation is almost the same as the

TABLE II
SOLUTIONS OF THE NON-CONVEX PFR-OPF AND ITS SDP RELAXATION FOR THE THREE IEEE TEST SYSTEMS

Solution & Performance	IEEE 30-Bus System				IEEE 57-Bus System				IEEE 118-Bus System			
	Baseline	4 UPFCs	2 PFRs	Full PFRs	Baseline	6 UPFCs	3 PFRs	Full PFRs	Baseline	13 UPFCs	5 PFRs	Full PFRs
ε_r	0	0.1	0.1	0.1	0	1	0.1	0.1	0	0.1	0.1	0.1
ε_s	0.1	0.1	0.1	0.1	1.2	0.1	0.1	0.1	0.1	0.02	0.01	0
λ_{opt} by SDP	1.034	1.650	1.656	1.658	1.076	1.538	1.539	1.546	2.036	2.286	2.291	2.302
λ_{opt} by NLP	1.034	1.650	1.656	1.658	1.077	1.539	1.539	1.546	2.037	2.291	2.291	2.302
Accuracy	100%	100%	100%	100%	99.9%	99.9%	100%	100%	99.9%	99.8%	100%	100%
Enhancement	-	59.6%	60.2%	60.3%	-	42.9%	42.9%	43.5%	-	12.5%	12.5%	13.0%

TABLE III
SOLUTIONS OF THE NON-CONVEX PFR-OPF AND ITS SDP RELAXATION FOR THE SEVEN MODELS OF THE POLISH SYSTEMS

System	Baseline			Some PFRs					Full PFRs			
	λ_{opt} by SDP	λ_{opt} by NLP	Accuracy	λ_{opt} by SDP	λ_{opt} by NLP	Accuracy	Penetration	Enhancement	λ_{opt} by SDP	λ_{opt} by NLP	Accuracy	Enhancement
PL-2383wp	1.014	1.015	99.9%	1.025	1.026	99.9%	4.11%	1.1%	1.030	1.030	100%	1.5%
PL-2736sp	1.095	1.098	99.7%	1.431	1.431	100%	4.27%	30.3%	1.501	1.501	100%	36.7%
PL-2737sop	1.275	1.276	99.9%	1.894	1.894	100%	4.60%	48.4%	1.987	1.987	100%	55.7%
PL-2746wop	1.289	1.292	99.8%	1.486	1.488	99.9%	1.97%	15.2%	1.554	1.557	99.8%	20.5%
PL-2746wp	1.111	1.111	100%	1.250	1.250	100%	1.97%	12.5%	1.270	1.272	99.8%	14.5%
PL-3012wp	1.080	1.083	99.7%	1.149	1.149	100%	1.99%	6.1%	1.161	1.161	100%	7.2%
PL-3120sp	1.117	1.117	100%	1.228	1.228	100%	5.22%	9.9%	1.253	1.253	100%	12.2%

λ_{opt} by the non-convex PFR-OPF problem for each of the scenarios. This suggests that the proposed SDP relaxation can obtain nearly optimal results of the PFR-OPF problem. While the penalization techniques are applied to pursue a rank-1 solution, the SDP relaxation can still obtain solutions which are nearly optimal. In addition, it does not need a careful choice of the initial solution, which is necessary for the NLP method, to yield a good solution of the non-convex PFR-OPF problem.

Fig. 6 demonstrates the evolution of the system loadability as the number of PFRs or UPFCs allocated in the network increases. The results indicate that with just a very small proportion of the buses or branches installed with PFRs or UPFCs, the power network can already benefit from a substantial improvement of loadability. Meanwhile, the marginal enhancement of loadability by adding a PFR or UPFC to the network decreases quickly as the number of PFRs and UPFCs available in the network increases. While the observation on the UPFC allocation matches with the existing findings on the allocation problem of FACTS devices [31], our study further reveals that the allocation of PFRs also possesses a similar pattern. Furthermore, when we revisit the allocation results in Fig. 6, Tables I and II together, we can see that the locations of the UPFCs involves more buses than that of the PFRs to achieve similar loadability enhancement. Hence, the labor cost for installation of the PFRs may be lower than that of the UPFCs. Nonetheless, a comprehensive evaluation model is necessary to make the most cost-effective decision.

F. Tractability for Large Systems

In this section, we investigate the numerical performance of the SDP relaxation and the penalization techniques in the large power networks with up to 3000 buses. Tables III and IV summarize the results of the seven models of the Polish power systems [34]. In Tables III and IV, the abbreviations

TABLE IV
COMPUTATION TIMES (SOLVER TIME IN SECONDS) OF THE NON-CONVEX PFR-OPF AND ITS SDP RELAXATION

System	Baseline		Some PFRs		Full PFRs	
	SDP	NLP	SDP	NLP	SDP	NLP
PL-2383wp	62.6	24.1	68.3	82.9	95.7	101.3
PL-2736sp	120.4	46.3	111.6	136.9	171.9	118.0
PL-2737sop	113.9	38.0	102.6	99.6	161.2	129.1
PL-2746wop	77.8	45.5	97.6	114.6	157.9	148.7
PL-2746wp	129.1	59.2	128.6	107.9	197.5	155.1
PL-3012wp	93.5	62.9	72.9	128.1	170.1	141.9
PL-3120sp	100.3	42.9	74.8	126.0	158.3	176.5

"PL," "s," "w," "op," and "p" stand for "Polish," "summer," "winter," "off-peak," and "peak," respectively. The scenario of the system with "some PFRs" is obtained by adding PFRs to the system so that the loadability is at least 95% of the maximum reachable loadability, which is similar to the scenario definition in Section V-C. "Penetration" represents the number of PFRs added to the system in that scenario to the number of buses. Other terms in Tables III and IV have the same meanings as those in Table II. To focus on the scalability of the algorithm, the results with PFC placement are not presented. For each of the test cases, we apply the procedure for determining the penalty coefficients ε_r and ε_s presented in Section V-D to obtain a rank-1 solution to the relaxed PFR-OPF problem in (33) so that the results are physically meaningful.

As shown in Table III, the proposed SDP relaxation can obtain optimal or near-optimal solutions for all of the seven large networks. Both the NLP and the SDP approaches can scale well. Each of the seven networks, except the PL-2383wp system, is able to benefit from significant loadability enhancement ranging from 7.2% to 20% by installing PFRs at only a small proportion of the buses in the network. Considering the diversities of the seven test systems in terms of network

sizes, loading conditions, i.e., off-peak and peak, and seasons, i.e., summer and winter time, the results indicate that the PFR integration is able to bring remarkable improvement of loadability in most practical scenarios. Furthermore, while the SDP relaxation alone may not be adequate to obtain practical solutions to the PFR-OPF problem, some remedial approaches, such as the penalization techniques adopted in this work, can be developed to improve the quality of the solutions and solve the problem to global or near-global optimality. Therefore, the convex relaxation approach can serve as a good alternative to the NLP approach and certify global optimality of the solutions. As an important future work, we will work on more sophisticated approaches, such as high-order moment relaxation, to further improve the exactness and numerical performance of the convex relaxation of the PFR-OPF problem.

The corresponding computation times of the NLP and the SDP approaches are reported in Table IV. Both approaches converge within two hundred seconds in all the test cases. It can be observed that, except for the baseline scenario, the computation times of the two approaches in each test case do not have a big difference in general. As for the baseline scenario, the NLP approach requires less time than the SDP approach in each test case. However, as PFRs are added to the OPF problem, the NLP approach exhibits an obvious and consistent increase in the computation times for each test system due to the increase in problem size and nonlinearity brought by the control variables of PFRs. On the other hand, since the dominant computational complexity of the SDP approach comes from the SDP constraints [18], the introduction of PFRs has a less significant effect on the computation time for the SDP approach than for the NLP approach. For each of the seven networks, the computation time of the "full-PFRs" scenario is higher than those of the baseline and "some-PFRs" scenarios. This agrees with the intuition because the PFR-OPF problem in the "full-PFRs" scenario has the highest computational complexity among various penetrations of PFRs.

VI. Conclusions

An OPF framework incorporated with PFRs is proposed to facilitate the theoretical study and optimization on power flow routing. First, the generic architecture with a load flow model of a PFR is proposed to characterize the desired functions of the PFR. Then, we formulate the PFR-incorporated OPF problem which extends the conventional OPF by augmenting the controllable ranges of terminal voltages. The SDP relaxation of the original non-convex PFR-OPF is derived to pursue global optimality and computational benefits. Our numerical study on the assessment of the system loadability shows that the integration of PFRs and PFCs to the power network can improve the loadability sigificantly, and that the proposed SDP relaxation succeeds in obtaining the optimal or near-optimal solution of the PFR-OPF problem. Moreover, the SDP approach helps certify that the local NLP approach finds the global optimums in all the test cases. Future work will generalize the SDP relaxation to a moment relaxation of the PFR-OPF problem, and further explore other potential advantages of power flow routing, such as extending the PFR-OPF framework to the corrective SCOPF scenario, and the coordinated and dynamic control of PFRs and PFCs to maintain the power balance and stability of the power network.

References

[1] R. Kandula, A. Iyer, R. Moghe, J. Hernandez, and D. Divan, "Power router for meshed systems based on a fractionally-rated back-to-back converter," *IEEE Trans. Power Electron.*, vol. 29, no. 10, pp. 5172–5180, Oct. 2014.

[2] H. Chen, A. Iyer, R. Harley, and D. Divan, "Dynamic grid power routing using controllable network transformers (CNT) with decoupled closed-loop controller," *IEEE Trans. Ind. Appl.*, vol. 51, no. 3, pp. 2361–2372, May 2015.

[3] N.G. Hingorani, L. Gyugyi, and M. El-Hawary, *Understanding FACTS: concepts and technology of flexible AC transmission systems*. Piscataway, NJ: IEEE Press, 2000.

[4] P. Nguyen, W. Kling, and P. Ribeiro, "Smart power router: a flexible agent-based converter interface in active distribution networks," *IEEE Trans. Smart Grid*, vol. 2, no. 3, pp. 487–495, Sep. 2011.

[5] J.J. Thomas and S. Grijalva, "Flexible security-constrained optimal power flow," *IEEE Trans. Power Syst.*, vol. 30, no. 3, pp. 1195–1202, May 2015.

[6] A. Sánchez-Squella, R. Ortega, R. Griño, and S. Malo, "Dynamic energy router," *IEEE Control Systems*, vol. 30, no. 6, pp. 72–80, Dec. 2010.

[7] X. She and A. Huang, "Solid state transformer in the future smart electrical system," in *Proc. IEEE PES General Meeting*, Jul. 2013.

[8] M. Noroozian, L. Angquist, M. Ghandhari, and G. Andersson, "Use of UPFC for optimal power flow control," *IEEE Trans. Power Del.*, vol. 12, no. 4, pp. 1629–1634, Oct. 1997.

[9] Y. Xiao, Y. H. Song, and Y. Z. Sun, "Power flow control approach to power systems with embedded facts devices," *IEEE Trans. Power Syst.*, vol. 17, no. 4, pp. 943–950, Nov. 2002.

[10] J.A. Momoh, *Electric power system applications of optimization*. CRC Press, 2008.

[11] B. Stott and O. Alsaç, "Optimal power flow–basic requirements for real-life problems and their solutions," in *Proc. SEPOPE XII Symp.*, Jul. 2012.

[12] L. Platbrood, F. Capitanescu, C. Merckx, H. Crisciu, and L. Wehenkel, "A generic approach for solving nonlinear-discrete security-constrained optimal power flow problems in large-scale systems," *IEEE Trans. Power Syst.*, vol. 29, no. 3, pp. 1194–1203, May 2014.

[13] A. Castillo and R.P. O'Neill, "Survey of approaches to solving the ACOPF (OPF paper 4)," US Federal Energy Regulatory Commission, Tech. Rep., 2013.

[14] D. Phan and J. Kalagnanam, "Some efficient optimization methods for solving the security-constrained optimal power flow problem," *IEEE Trans. Power Syst.*, vol. 29, no. 2, pp. 863–872, Mar. 2014.

[15] J. Lavaei and S.H. Low, "Zero duality gap in optimal power flow problem," *IEEE Trans. Power Syst.*, vol. 27, no. 1, pp. 92–107, Feb. 2012.

[16] C. Josz, J. Maeght, P. Panciatici, and J.C. Gilbert, "Application of the moment-SOS approach to global optimization of the OPF problem," *IEEE Trans. Power Syst.*, vol. 30, no. 1, pp. 463–470, Jan. 2015.

[17] S.H. Low, "Convex relaxation of optimal power flow: Parts I & II," *IEEE Trans. Control Network Syst.*, vol. 1, no. 1, pp. 15–27, Mar. 2014.

[18] R. Madani, M. Ashraphijuo, and J. Lavaei, "Promises of conic relaxation for contingency-constrained optimal power flow problem," *IEEE Trans. Power Syst.*, vol. 31, no. 2, pp. 1297–1307, Mar. 2016.

[19] R. Madani, S. Sojoudi, and J. Lavaei, "Convex relaxation for optimal power flow problem: Mesh networks," *IEEE Trans. Power Syst.*, vol. 30, no. 1, pp. 199–211, Jan. 2015.

[20] D.K. Molzahn and I.A. Hiskens, "Sparsity-exploiting moment-based relaxations of the optimal power flow problem," *IEEE Trans. Power Syst.*, vol. 30, no. 6, pp. 3168–3180, Nov. 2015.

[21] D.K. Molzahn, C. Josz, I.A. Hiskens, and P. Panciatici, "A laplacian-based approach for finding near globally optimal solutions to OPF problems," arXiv:1507.07212 [math.OC], 2015.

[22] ——, "Solution of optimal power flow problems using moment relaxations augmented with objective function penalization," in *Proc. IEEE CDC*, Dec. 2015.

[23] B. Zhang, A.Y.S. Lam, A. Dominguez-Garcia, and D. Tse, "An optimal and distributed method for voltage regulation in power distribution systems," *IEEE Trans. Power Syst.*, vol. 30, no. 4, pp. 1714–1726, Jul. 2015.
[24] W.A. Bukhsh, A. Grothey, K.I.M. McKinnon, and P.A. Trodden, "Local solutions of the optimal power flow problem," *IEEE Trans. Power Syst.*, vol. 28, no. 4, pp. 4780–4788, Nov. 2013.
[25] J. Lin, V.O.K. Li, K.-C. Leung, and A.Y.S. Lam, "Architectural design and load flow study of power flow routers," in *Proc. IEEE Int. Conf. Smart Grid Commun. (SmartGridComm'14)*, Nov. 2014, pp. 43–48.
[26] S.Y. Hui, C.K. Lee, and F.F. Wu, "Electric springs – a new smart grid technology," *IEEE Trans. Smart Grid*, vol. 3, no. 3, pp. 1552–1561, Sep. 2012.
[27] Z. Akhtar, B. Chaudhuri, and S.Y.R. Hui, "Smart loads for voltage control in distribution networks," *IEEE Trans. Smart Grid*, 2015, to appear.
[28] B. Recht, M. Fazel, and P.A. Parrilo, "Guaranteed minimum-rank solutions of linear matrix equations via nuclear norm minimization," *SIAM Rev.*, vol. 52, pp. 471–501, Aug. 2010.
[29] R. Grone, C.R. Johnson, E.M. Sá, and H. Wolkowicz, "Positive definite completions of partial hermitian matrices," *Linear Algebra Appl.*, vol. 58, 1984.
[30] Power systems test case archive. University of Washington. [Online]. Available: http://www.ee.washington.edu/research/pstca/
[31] C. Duan, W. Fang, L. Jiang, and S. Niu, "FACTS devices allocation via sparse optimization," *IEEE Trans. Power Syst.*, vol. 31, no. 2, pp. 1308–1319, Mar. 2016.
[32] J. Guo, M.L. Crow, and J. Sarangapani, "An improved UPFC control for oscillation damping," *IEEE Trans. Power Syst.*, vol. 24, no. 1, pp. 288–296, Feb. 2009.
[33] A. Rajabi-Ghahnavieh, M. Fotuhi-Firuzabad, M. Shahidehpour, and R. Feuillet, "UPFC for enhancing power system reliability," *IEEE Trans. Power Del.*, vol. 25, no. 4, pp. 2881–2890, Oct. 2010.
[34] R.D. Zimmerman, C.E. Murillo-Sánchez, and R.J. Thomas, "MATPOWER: Steady-state operations, planning and analysis tools for power systems research and education," *IEEE Trans. Power Syst.*, vol. 26, no. 1, pp. 12–19, Feb. 2011.
[35] A. Wächter and L. T. Biegler, "On the implementation of an interior-point filter line-search algorithm for large-scale nonlinear programming," *Math. Program.*, vol. 106, no. 1, pp. 25–57, 2006.
[36] J. Bezanson, A. Edelman, S. Karpinski, and V.B. Shah, "Julia: A fresh approach to numerical computing," arXiv:1411.1607v4 [cs.MS], 2015.
[37] MOSEK ApS, *The MOSEK optimization toolbox for MATLAB manual. Version 7.1 (Revision 28)*, 2015. [Online]. Available: http://docs.mosek.com/7.1/toolbox/index.html
[38] M. Grant and S. Boyd, "CVX: Matlab software for disciplined convex programming, version 2.1," http://cvxr.com/cvx, Mar. 2014.
[39] F. Alhasawi and J. Milanović, "Techno-economic contribution of facts devices to the operation of power systems with high level of wind power integration," *IEEE Trans. Power Syst.*, vol. 27, no. 3, pp. 1414–1421, Aug. 2012.

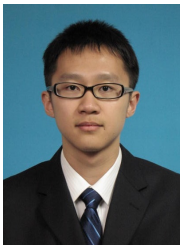

Junhao Lin (S'13) received the B.Eng. degree in electronic engineering from Tsinghua University, Beijing, China in 2012. He is currently pursuing the Ph.D. degree at the University of Hong Kong under supervision of Prof. V. O. K. Li and Dr. K.-C. Leung. His research interests are in optimization and control of smart grids, including power flow routing, vehicle-to-grid, demand response, energy storage, and integration of renewable energy sources.

Victor O.K. Li (S'80–M'81–F'92) received SB, SM, EE and ScD degrees in Electrical Engineering and Computer Science from MIT in 1977, 1979, 1980, and 1981, respectively. He is Chair Professor of Information Engineering and Head of the Department of Electrical and Electronic Engineering at the University of Hong Kong (HKU). He has also served as Assoc. Dean of Engineering and Managing Director of Versitech Ltd., the technology transfer and commercial arm of HKU. He served on the board of China.com Ltd., and now serves on the board of Sunevision Holdings Ltd., listed on the Hong Kong Stock Exchange. Previously, he was Professor of Electrical Engineering at the University of Southern California (USC), Los Angeles, California, USA, and Director of the USC Communication Sciences Institute. His research is in the technologies and applications of information technology, including clean energy and environment, social networks, wireless networks, and optimization techniques. Sought by government, industry, and academic organizations, he has lectured and consulted extensively around the world. He has received numerous awards, including the PRC Ministry of Education Changjiang Chair Professorship at Tsinghua University, the UK Royal Academy of Engineering Senior Visiting Fellowship in Communications, the Croucher Foundation Senior Research Fellowship, and the Order of the Bronze Bauhinia Star, Government of the Hong Kong Special Administrative Region, China. He is a Registered Professional Engineer and a Fellow of the Hong Kong Academy of Engineering Sciences, the IEEE, the IAE, and the HKIE.

Ka-Cheong Leung (S'95–M'01) received the B.Eng. degree in Computer Science from the Hong Kong University of Science and Technology, Hong Kong, in 1994, the M.Sc. degree in Electrical Engineering (Computer Networks) and the Ph.D. degree in Computer Engineering from the University of Southern California, Los Angeles, California, USA, in 1997 and 2000, respectively. He worked as Senior Research Engineer at Nokia Research Center, Nokia Inc., Irving, Texas, USA from 2001 to 2002. He was Assistant Professor at the Department of Computer Science at Texas Tech University, Lubbock, Texas, USA, between 2002 and 2005. Since June 2005 he has been with the University of Hong Kong, Hong Kong, where he is currently Assistant Professor at the Department of Electrical and Electronic Engineering. His research interests include power flow routing, transport layer protocol design, congestion control, wireless packet scheduling, and vehicle-to-grid (V2G).

Albert Y.S. Lam (S'03–M'10) received the BEng degree (First Class Honors) in Information Engineering and the PhD degree in Electrical and Electronic Engineering from the University of Hong Kong (HKU), Hong Kong, in 2005 and 2010, respectively. He was a postdoctoral scholar at the Department of Electrical Engineering and Computer Sciences of University of California, Berkeley, CA, USA, in 2010–12, and now he is a research assistant professor at the Department of Electrical and Electronic Engineering of HKU. He is a Croucher research fellow. His research interests include optimization theory and algorithms, evolutionary computation, smart grid, and smart city.